

Study of Preparation, Growth Mechanism and Catalytic Performance of Carbon Based Embedded Silver Nano Composite Materials

Pengpeng Jiang, Jiao Liu, Yingxin Huang, Xiaohong Jiang*, Lude Lu

International Chinese-Belarusian scientific laboratory on vacuum-plasma technology, Nanjing University of Science and Technology, Nanjing 210094, China

Article info

Received:
15 June 2016

Received in revised form:
23 August 2016

Accepted:
24 October 2016

Keywords:

carbon materials
nanoparticles
composite materials
photocatalytic performance

Abstract

Novel and stable carbon based embedded silver nano composite materials (Ag/CSs) were successfully prepared by a facile one-pot hydrothermal method with trioctylamine (TOA) as soft template and stabilizer. These as-prepared Ag/CSs exhibit well-defined shape and relatively uniform size with an average diameter of 1.5 μm and uniformly embedded Ag nanoparticles about 5 nm. The proper proportion of glucose, AgNO_3 and TOA is the key to the common growth of hydrothermal carbon materials and silver nanoparticles in an embedded way. Besides, the thickness of carbon sphere matrix and the size of Ag particles can be tailored precisely by adjusting the experimental parameters. In order to facilitate comparative analysis, carbon spheres (CSs) without Ag particles embedded were also prepared with glucose under the same hydrothermal reaction conditions. The composition, structure and morphology of the as-prepared Ag/CSs and CSs were confirmed by X-ray powder diffraction (XRD), FT-IR spectroscopy, Raman spectrum, Transmission electron microscopy (TEM) and scanning electron microscopy (SEM). In addition, the possible formation mechanism of the Ag/CSs has been proposed based on experimental evidences. Finally, the as-prepared Ag/CSs and CSs were used as catalysts in the experiments of photocatalytic degradation of methylene MB in water under visible light irradiation and the high efficiency of photocatalytic performance of Ag/CSs has been verified.

1. Introduction

Silver nanoparticles have received considerable attention for many years because of its fascinating catalytic performance and other widespread use in applications related to photonics, information storage, chemical/biological sensing and surface-enhanced Raman scattering (SERS) [1]. In an effort to tailor their properties and improve their performance in applications, people have developed various chemical methods for generating silver with different morphologies [2]. However, they would often congregate during the photocatalytic reaction process, for nano-sized metal particles are active and prone to coalesce due to Van der Waals force and high surface energy unless they are protected.

The structure of supporting materials plays an important role in the activity of the catalyst [3]. It is well known that hydrothermal CSs have been

widely studied by both academic and industrial researchers since they have many interesting properties, such as a very special shape, low density, high specific surface area, high chemical and structural stabilities [4]. These excellent properties make it widely used in many fields. For example, it is often designed to be applied in gas adsorbent [5], catalyst supports [6], lithium-ion batteries [7], super capacitor [8] and so on.

In the early stage, the preparation methods of silver-carbon composites mainly include high temperature pyrolysis method and chemical vapor deposition method. It is obviously that these methods are difficult to realize the design of composite materials with special structure. In recent years, the hydrothermal reduction carbonization method, using water as the reaction medium carbohydrate as a carbon source and a reducing agent, is widely used. Compared with other techniques,

*Corresponding author. E-mail: jiangxh24@njjust.edu.cn

the hydrothermal reduction method has mild reaction conditions, low energy consumption and simple operation, which can achieve the morphology control of the composite materials. For instance, hydrothermal carbon spheres with metal nanoparticles doping are attracting increased interest [9–11] because hydrothermal carbonaceous materials own abundant hydroxyl groups, which can help to load with noble-metal nanoparticles and make them possible to integrate differently sized noble-metal nanoparticles with layered structures [12]. However, these noble-metal nanoparticles were loaded on the CSs surface by in-situ reduction after the as-prepared CSs were dispersed in AgNO_3 aqueous solutions, which can not to solve the problem of silver nanoparticles prone to be oxidized easily.

In order to prevent the aggregation and oxidation of silver nanoparticles, various methods of preparing Ag-carbon core-shell structure are springing up [13–15]. The silver kernel is effectively prevented from being oxidized by air. However, the aggregates of silver group overall encapsulated in carbon based, which limited its specific surface area. If these core-shell materials used as catalyst, its catalytic activity must be weakened for the thick carbonaceous shell.

Suppose that silver nanoparticles were equably embedded in the carbonaceous matrix, the composites would differ in several aspects:

1. Silver nanoparticles were largely prevented from agglomeration because porous carbonaceous matrix provide silver nanoparticles with a larger space, which makes silver nanoparticles more dispersive and stable.

2. Silver nanoparticles embedded in the carbonaceous still can be protected from oxidation to a certain extent and keep catalytic activity.

3. The porous structure of carbonaceous makes silver nanoparticles in full touch with the reactant. As a result, the catalytic efficiency is improved.

4. The embedded composite structure is beneficial to change the energy of reaction intermediate state and the distribution of charge, leading to the decrease of the reaction activation energy and the increase of the reaction conversion and selectivity.

In this paper, glucose and silver nitrate was chosen as raw materials, TOA was used as soft template to prepare carbon-based embedded silver nano composites with different morphologies and structures via one-pot hydrothermal reduction method. The silver nanoparticles were uniformly imbedded in the loose carbonaceous matrix during the process of polymerization and carbonization

of glucose. At the same time, this common growth pattern means that the crystal growth of silver would be limited by the carbonaceous shell. The thickness of carbonaceous matrix and the size of embedded silver particles can be controlled in the growth process. The structure of the composites is "embedded" mode, which is completely different from the "load" and the "encapsulated" composite way. In addition, this "embedded" mode can prevent the oxidation of silver nanoparticles to a certain extent, greatly increase the specific surface area and improve the catalytic activity. The formation mechanism and growth models of Ag/CSs were established. Finally, the as-prepared Ag/CSs with high degradation efficiency and photocatalytic activities were validated in the experiment of decomposing the methylene blue (MB) in water and irradiated by visible light.

2. Experimental

2.1. Materials

Silver nitrate (AgNO_3 , AR), glucose (AR), and ethanol (AR) were purchased from Sinopharm Chemical Reagent Co. Ltd. Methylene blue (MB) and Trioctylamine (TOA, 90%) were obtained from Sigma-Aldrich. All the chemicals were used as received without further purification. Deionized water was used throughout all the experiments.

2.2. Synthesis of Ag/CSs

In a typical experiment, 0.076 g of AgNO_3 and 1.29 g of glucose were dissolved in 30 ml deionized water, respectively. These two solutions were mixed under vigorous stirring, and then 1.0 ml of TOA was added into the mixture. The mixture of reactants was ultrasonic-treated for 10 min to form the emulsion. Then the emulsion was quickly transferred to 100 ml Teflon-lined autoclave and sealed for 12 h at 180 °C. After the reaction, the autoclave was cooled to room temperature in air. The resulting suspension was purified by repeated centrifugation/redispersion cycles with deionized water and anhydrous ethanol until supernatant became a clear solution. And the precipitate was collected after centrifugation. Finally, the resultant precipitate was vacuum-dried at 60 °C for 12 h.

2.3. Synthesis of hydrothermal carbon spheres

CSs were prepared by hydrothermal method

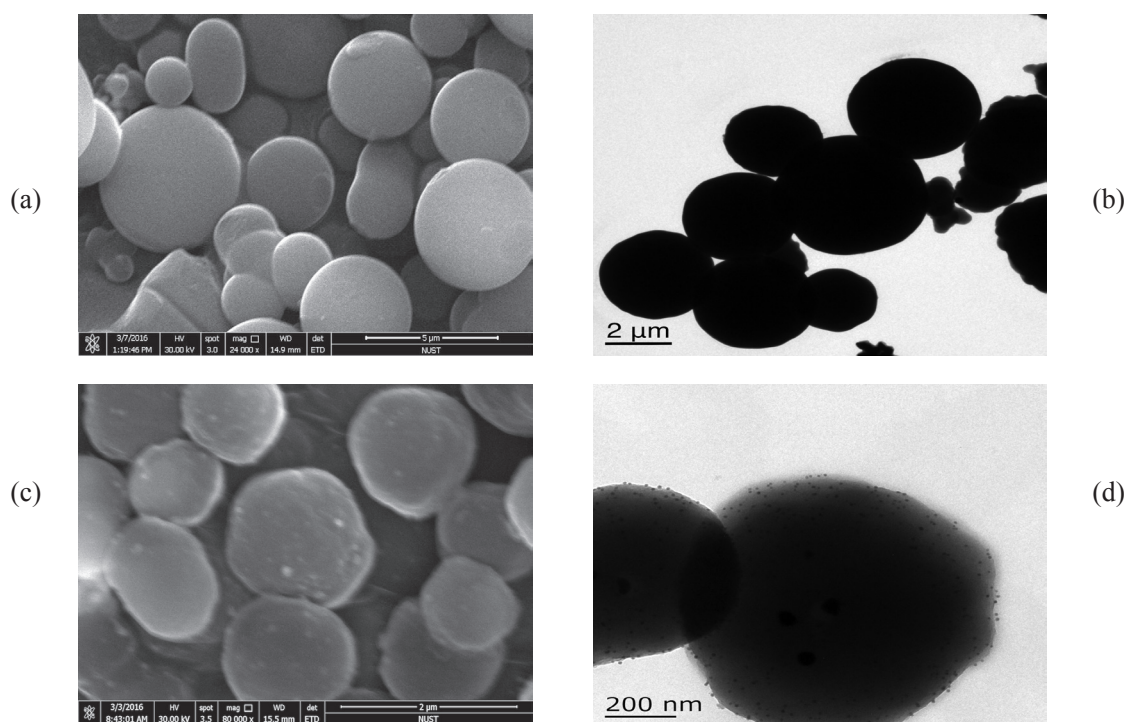


Fig. 1. SEM and TEM images of as-synthesized CSs (a and b) and Ag/CSs (c and d).

with glucose as the precursor. Typically, 2.58 g of glucose were dissolved in 60 ml deionized water, and then 1.0 ml of TOA was added into the glucose solution. In order to ensure the objectivity of results, all of the following steps are aligned with the preparation method of Ag/CSs.

2.4. Characterization

The structure characterization of Ag/CSs was carried out on X-ray (German Bruker AXSD8 advance). FT-IR spectra of particles were obtained using a Thermo Scientific Nicolet IS-10 spectrometer. Raman spectra were recorded with a Britain Renishaw InVia Raman spectrometer. Morphology studies were carried out on a scanning electron microscope (HITACHI S-4800) operating at accelerating voltage of 30 kV and a transmission electron microscope (FEI F-30). Quantitative determination of MB was performed by measuring the absorption at 663 nm with a U-222 UV-Vis spectrophotometer.

3. Results and discussion

3.1. Structure and morphology of as-prepared CSs and Ag/CSs

Typical SEM and TEM images of the formed CSs and Ag/CSs are shown in Fig. 1. From the SEM picture (Fig. 1a) we can see that the surface

of carbon spheres is very smooth if AgNO_3 absent from the reaction. However, the average size of carbon spheres is too thick to penetrate for electrons, thus it's hard to see the internal structure of the carbon spheres (Fig. 1b). The internal and external structures are completely different, if the amount of glucose was halved and 0.007 M of AgNO_3 was added at the beginning of reaction. The Fig. 1c and 1d are SEM and TEM images of the as prepared Ag/CSs. Some obviously little bright spots on the surface and many black dots inside of carbon spheres can be seen, respectively. It is a very intuitive proof of silver nanoparticles are embedded in carbon spheres. Furthermore, the average particle size of the embedded silver nanoparticles was only 5 nm and very close to the size of the clusters, which may give new properties to Ag/CSs.

3.2. Comparative analysis of chemical component for as-prepared CSs and Ag/CSs

Figure 2 shows the XRD and Raman patterns of as-synthesized CSs and Ag/CSs. There is an obvious broad peak at around 24° in Fig. 2a, which indicates an amorphous phase and is corresponded to the carbonaceous composition of the CSs. In contrast, the peak shifts to the left slightly in the Ag/CSs and the intensity of the peak that belongs to the carbon decreases. It means that the disorder

of carbonaceous composition increased, considering that silver nanoparticles were imbedded in the carbonaceous matrix. In addition, four distinct diffraction peaks were clearly observed at 2θ value of 38.14° , 44.32° , 64.48° and 77.45° corresponding to the (111), (200), (220) and (311) crystalline planes of Ag, respectively, which is in good agreement with the reported data (JCPDS #87-0720). It means that the AgNO_3 has already been reduced to Ag by glucose. Those observations confirm the successful preparation of Ag/CSs hybrid. Additionally, in general, Ag nanoparticles are easy to be oxidized in the synthesis and washing processes, but no silver oxide phase such as Ag_2O is detected. This is due to the fact that the Ag nanoparticles are imbedded in the matrix of CSs, which protects the Ag nanoparticles from the oxidation effectively.

As shown in Fig. 2b, two carbon-related broad peaks in Raman spectra are exhibited; one is around 1384 cm^{-1} (D-band), and the other is around 1595 cm^{-1} (G-band), which includes the bonding information of sp^2 and sp^3 site vibrations. This reveals

that carbon-containing materials exist around the silver nanoparticles and they are amorphous in nanostructure. The G-band is originated from the bond stretching of all pairs of sp^2 atoms in both rings and chains, and the D-band is originated from the breathing modes of sp^3 atoms in rings induced by disordered-activated aromatic modes of A1 symmetry [16]. By comparing of the peak intensities from Ag/CSs and CSs, we can find that the peak intensity of the former is much more than that of the latter. This may due to the Surface Enhancement Raman Scattering effect of Ag nanoparticles [17]. In addition, both spectrum can be divided into two peaks (G-peak and D-peak) by Gaussian fitting. According to the area ratio of D-peak to G-peak (I_D/I_G) in Fig. 3, the fitting peak area ratio of Ag/CSs is 3 times as much as CSs, which means the crystallinity of carbonaceous matrix was weakened after silver nanoparticles imbedded. Above Raman analysis results not only do further confirm the existence of carbon in the Ag/CSs, but also accordance with the conclusions obtained from XRD spectra.

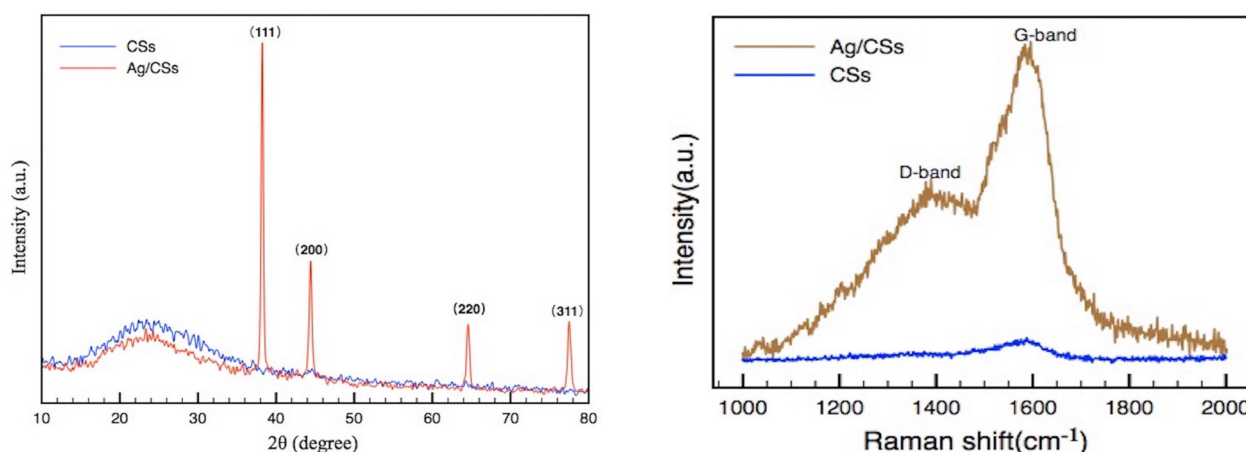


Fig. 2. XRD pattern (a) and Raman spectra (b) of as-synthesized CSs and Ag/CSs.

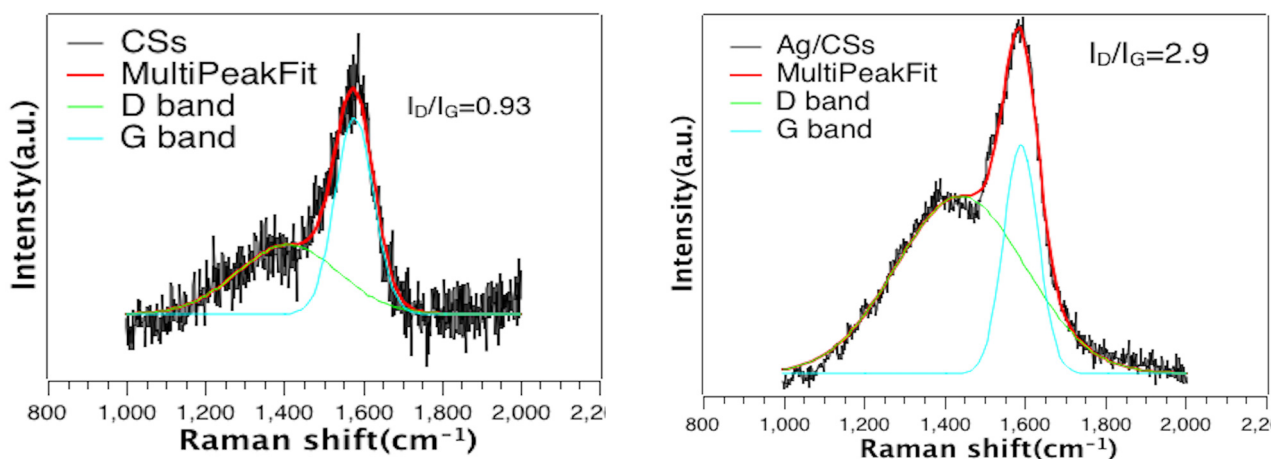


Fig. 3. Gaussian fitting spectrum (G-peak and D-peak) of CSs and Ag/CSs.

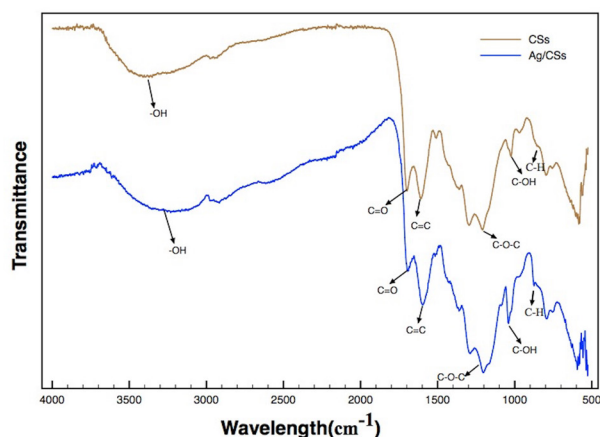


Fig. 4. FTIR spectra of as-synthesized CSs and Ag/CSs.

The two FTIR spectra of CSs and Ag/CSs are shown in Fig. 4. It could be observed that the functional groups of Ag/CSs varied greatly owing to the silver nanoparticles imbedded. From the spectra of CSs, we can see the bands at 3350 and 1045 cm^{-1} , are due to -OH stretching vibrations, C-OH stretching and -OH bending vibrations, which indicates the existence of hydroxyl groups. The vibration band at 1692 cm^{-1} is attributed to C=O vibrations. The band at 880 cm^{-1} is corresponding to the vibration of aromatic C-H groups. What's more, the characteristic vibration peaks of benzene framework positioned at 1600, 1558, 1507, 1453 cm^{-1} unambiguously indicates the existence of benzene ring structure in the carbonaceous shell. Comparison with CSs, the C=C vibration peak, C-O-C vibration peak and C-OH vibration peak of Ag/CSs are greatly enhanced, which confirms the idea that Ag nanoparticles can catalyze the aromatization of glucose during hydrothermal treatment [18]. While, it should be noticed that the C=O vibration peak is weakened conversely. This may reveal that silver nanoparticles and carbon matrix were bonding with coordinated bond.

3.3. The possible formation mechanism of the Ag/CSs

The formation mechanism of Ag/CSs can be summarized in Fig. 5. After stirring and ultrasonic treatment, TOA liquids can be dispersed in the water phase to form an emulsion. At this time, Ag^+ outside the droplet forms Ag-amine complex. When the temperature in autoclave is above 80 $^{\circ}\text{C}$, Ag^+ will be reduced by glucose to form Ag nanoparticles. Meanwhile, these silver nanoparticles will be wrapped by TOA droplet, which effectively prevent the aggregation and growth of

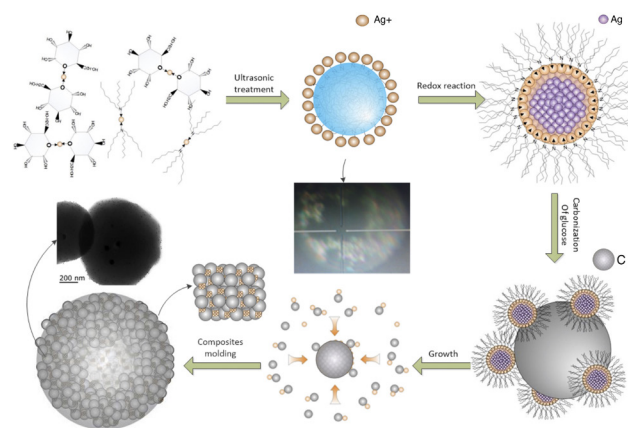


Fig. 5. The possible formation mechanism of Ag/CSs.

silver nanoparticles. When temperature continues to increase, glucose began to be carbonated. The generated carbon cores preferentially grow on the surface of the silver nanoparticles along with other Ag nanoparticles. Finally, due to the surface energy, most of Ag/CSs has grown into a spherical shape.

3.4. The photocatalytic performance of the Ag/CSs

The photocatalytic activities of the as-prepared products were evaluated by decomposing the methylene blue (MB) in water and irradiated by visible light. A 500W Xe lamp with a 420 nm cutoff filter was used as light source to provide visible light irradiation. Fifty milligram of photocatalyst was dispersed into 50 mL MB (10 mg L^{-1}) solution for photocatalytic examination. Prior to the visible light irradiation, the flask was kept in the dark for 30 min with continuous magnetic stirring to reach adsorption-desorption equilibrium. During irradiation, 3.5 mL of the suspension were collected after every 10 min, centrifuged to remove the catalyst and then quantitative determination of MB was performed by measuring the absorption at 663 nm with a U-222 UV-Vis spectrophotometer. As is shown in Fig. 6, degradation efficiency was calculated using C/C_0 , where C is the concentration of the remaining dye solution at each irradiated interval, and C_0 is the initial concentration. Degradation rate of Ag/CSs is very fast, most of MB was degraded only using an hour. On the one hand, the adsorption effect of carbon spheres provided a high-concentration environment to increase the reaction rate, on the other hand, silver nanoparticles imbedded in carbonaceous matrix has played a major role in catalysis.

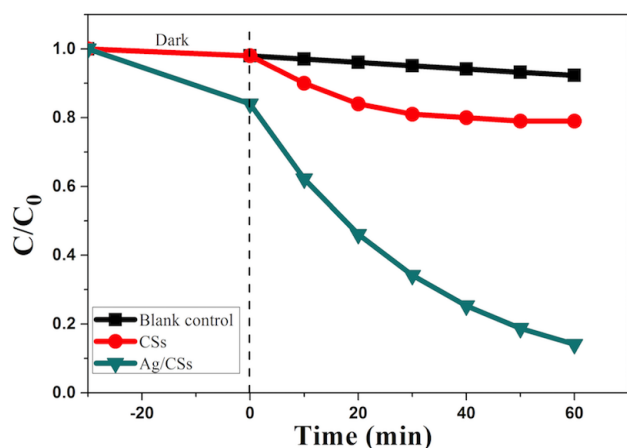


Fig. 6. The rate curves of photocatalytic degradation of methylene blue (MB) in water under visible light irradiation using the as-prepared products as catalysts.

4. Conclusion

In this paper, a kind of novel and stable Ag/CSs was successfully prepared by a simple one-pot hydrothermal technique. Ag nanoparticles were obtained from the reduction of silver nitrate under hydrothermal conditions by glucose, and the average particle size was only 5 nm, which was very close to that of clusters. These Ag nanoparticles acted as catalysts during the polymerization and carbonization of glucose and deepened its aromatization. The carbonaceous matrix of Ag/CSs can effectively protect Ag nanoparticles from oxidation and exhibits a stronger Raman scattering signal and a higher degree of disorder due to the embedding of Ag nanoparticles. In addition, Ag/CSs showed excellent catalytic performance in the experiment of photocatalytic degradation of methylene MB in water under visible light irradiation. What's more, there should be a lot of potential excellent performance to be excavated in other field, our work is only the beginning of the novel imbedded Ag/CSs.

Acknowledgements

This work was supported by the National Natural Science Foundation of China (51373077), 2015-2016 Intergovernmental Cooperation Projects in Science and Technology of the Ministry of Science and Technology of PRC (No. CB11-09 & CB11-11).

References

- [1]. Yanyun Ma, Weiyang Li, Eun Chui Cho, Zhiyuan Li, and Younan Xia, *Acs Nano* 4 (11) (2010) 6725–6734. DOI: 10.1021/nn102237c
- [2]. B.J. Wiley, S.H. Im, Z. Li, J. McLellan, A. Siekkinen and Y. Xia, *J. Phys. Chem. B* 110 (2006) 15666–15675. DOI: 10.1021/jp0608628
- [3]. Shu Ying Wu, Yun Sheng Ding, Xiao Min Zhang, Hai Ou Tang, Long Chen, and Bo Xuan Li, *J. Solid State Chem.* 2171 (2008) 2127–2132. DOI: 10.1016/j.jssc.2008.04.043
- [4]. N. Baccile, G. Laurent, F. Babonneau, F. Fayon, and M.M. Titirici, M. Antonietti, *J. Phys. Chem. C* 113 (2009) 9644–9654. DOI: 10.1021/jp901582x
- [5]. A. Chen, Y. Yu, Y. Zhang, W. Zang, Y. Yu, Y. Zhang, S. Shen, and J. Zhang, *Carbon* 80 (2017) 19–27. DOI: 10.1016/j.carbon.2014.08.003
- [6]. J. Wu, C. Jin, Z. Yang, J. Tian, and R. Yang, *Carbon* 82 (2015) 562–571. DOI: 10.1016/j.carbon.2014.11.008
- [7]. C. Galeano, J.C. Meier, M. Soorholtz, H. Bongard, C. Baldizzone, and K.J.J. Mayrhofer, *ACS CATAL* 4 (2014) 3856–3868. DOI: 10.1021/cs5003492
- [8]. J. Zhang, K. Wang, S. Guo, S. Wang, Z. Liang, and Z. Chen, *Acs Appl. MATER INTER* 6 (2014) 2192–2198. DOI: 10.1021/am405375s
- [9]. D. Lee, S.M. Kim, H. Jeong, J. Kim, and I.S. Lee, *Acs Nano* 8 (2014) 4510–4521. DOI: 10.1021/nn5020598
- [10]. X. Sun, and Y. Li, *J. Colloid Interface Sci.* 291 (2005) 7–12. DOI: 10.1016/j.jcis.2005.04.101
- [11]. H. Liu, X. Zhou, F. Wang, J. Ji, J. Liu, Z. Li, and Y. Jia, *Mater. Res. Bull.* 57 (2014) 280–286. DOI: 10.1016/j.materresbull.2014.05.021
- [12]. S. Tang, S. Vongehr, and X. Meng, *J. Phys. Chem.* 114 (2010) 977–982. DOI: 10.1021/jp9102492
- [13]. Sun Xiaoming, and Li Yadong, *Angew. Chem. Int. Ed.* 43 (2004) 597–601. DOI: 10.1002/anie.200352386
- [14]. S.H. Yu, X. Cui, L.L. Li, K. Li, B. Yu, M. Antonietti, and H. Cölfen, *Adv. Mater.* 16 (2004) 1636–1640. DOI: 10.1002/adma.200400522
- [15]. Li Dawei, Wu Shifa, and Wang Qiao, *J. Phys. Chem.* 116 (2012) 12283–12294. DOI: 10.1021/jp3018088
- [16]. F.X. Liu, and Z.L. Wang, *Surf. Coat. Technol* 203 (2009) 1829–1832. DOI: 10.1016/j.surfcoat.2009.01.008
- [17]. Dawei Li, Shifa Wu, Qiao Wang, Yongkuan Wu, Wei Peng, and Lujun Pan, *J. Phys. Chem. C* 116 (2012) 12283–12294. DOI: 10.1021/jp3018088
- [18]. X. Cui, M. Antonietti, and S. Yu, *Small* 2 (2006) 756–759. DOI: 10.1002/sml.200600047